

Hall ASICs with Integrated Magnetic Concentrators

Radivoje S. Popovic
EPFL-Swiss Federal Institute of Technology
Lausanne
CH-1015 Lausanne, Switzerland;
and
Christian Schott
SENTRON AG
Baarerstrasse 73, CH-6300 Zug, Switzerland
Email: radivoje.popovic@epfl.ch;
christian@sentron.ch

1. ABSTRACT

We describe new magnetic field sensors consisting of a combination of a CMOS Hall ASIC and an Integrated Magnetic Concentrator (in short IMC). The IMC converts an external magnetic field parallel with the chip surface locally into a field perpendicular to the surface. The perpendicular component of the magnetic field is then sensed by conventional planar Hall elements. A magnetic concentrator also functions as a passive magnetic amplifier and dramatically improves sensor performance. An IMC Hall ASIC combines the best characteristic of magnetoresistive (MR) sensors and conventional Hall ASICs. Application examples of this new technology include an integrated magnetic sensor with the world-record sensitivity of 3000 V/T and offset of 3 μ T; the first integrated current sensor; and the first integrated magnetic angular position sensor with the precision of 0.5° over 360°.

2. INTRODUCTION

The idea of combining a semiconductor magnetic field sensor with ferromagnetic structures came to many researchers in the past. Probably the first report on the subject was published back in 1955 [1]. In order to amplify the magnetic field “seen” by an InSb Hall plate, the authors put the Hall plate in the air gap between two long ferromagnetic rods. In this way they considerably increased the effective sensitivity and the resolution of the Hall element and could measure quasi-static magnetic fields down to milli-gauss range. The operation of this device is based on the following well-known effect: if a ferromagnetic rod is placed in a magnetic field parallel with the long axis of the rod,

the rod tends to collect the magnetic field lines in itself: it operates as a magnetic flux concentrator. Similar macroscopic systems Hall sensor – Magnetic concentrators, made of discrete components, were investigated also by other researchers [2] – [4]. We developed a first hybrid micro-system Hall sensor – Magnetic concentrators [5] which became a part of a commercially available product. The highest reported detectivity limit of a combination Hall sensor – Magnetic concentrators is as low as 10 pT [3].

In [3] we find also a report on an attempt to incorporate ferromagnetic material into the package of a Hall device. This idea is also presented in [6], and is now used in several commercially available Hall magnetic sensors.

To the best of our knowledge, the idea of using an integrated combination of a semiconductor magnetic micro-sensor and a thin ferromagnetic layer was mentioned for the first time in a patent [7].

In this paper we describe integrated combinations of Hall sensors and magnetic flux concentrators. We shall refer to such Integrated Magnetic Concentrators in short as IMC. As in the case of the conventional applications of magnetic concentrators [1] - [5], we use the IMCs as passive magnetic amplifiers. However, the structure of our concentrators is different: an IMC is planar, which allows an easy integration on a semiconductor wafer. Moreover, a planar IMC changes the sensitivity direction of the sensor: whereas a conventional Hall ASIC responds to a magnetic field perpendicular to the chip surface, a Hall ASIC with IMC responds to a magnetic field parallel with the chip surface.

We shall first describe two basic structures, one with so-called twin magnetic flux concentrators and the other with a single magnetic flux concentrator. Then we shall discuss their performance and briefly present a few application examples.

Some parts of this paper were presented at two recent conferences [8], [9].

3. TWIN MAGNETIC FLUX CONCENTRATORS

The idea of the integrated twin magnetic flux concentrators [10] is illustrated in Figure 1a). Obviously, the idea is inspired by the conventional configuration of the combination

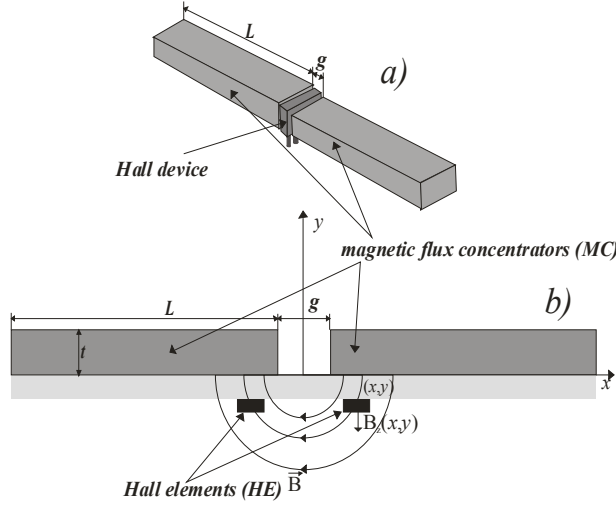


Figure 1 Comparison of a conventional (a) and an integrated (b) combination Hall magnetic sensor – magnetic flux concentrators: a) the Hall device is placed in the air gap between the two flux concentrators; b) two Hall elements are placed under the planar magnetic concentrators [11].

Hall magnetic sensor – rod-like magnetic concentrators (MC) – Fig. 1a). The key difference is, however, that the Hall element in (b) is placed not inside, but near the air gap and under the concentrators. In this way, we can use conventional planar integrated Hall elements and we can define by photolithography the shape of IMCs and the mutual positions in the system IMCs – Hall elements.

The integrated magnetic flux concentrators consist of a high-permeability and low-coercive-field (very soft) ferromagnetic layer, bonded on the Hall sensor chip surface. The layer is structured such, that a narrow air gap is created approximately in the middle of the chip. Figure 2 shows the distribution of the magnetic field lines around the MCs. The MCs “suck in” the magnetic field lines and convert locally the magnetic field parallel with chip surface into a magnetic field perpendicular to the chip surface. The perpendicular component of the magnetic field is the strongest near

the gap. There we place the Hall elements [11]. We use two Hall elements because two equivalent places, one under each concentrator, are available and so we increase the signal to noise ratio. The Hall plates below the different concentrators see the useful magnetic field in opposite direction. So the system is insensitive to an external field component perpendicular to the chip surface [12].

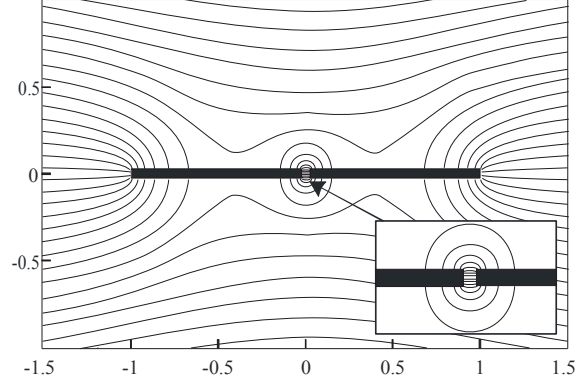


Figure 2 The result of a two-dimensional simulation of twin planar MCs introduced into a homogenous magnetic field parallel with the MC-plane [11].

In order to obtain an intuitive insight into the behavior of the magnetic concentrators, we shall now perform an approximate two-dimensional analysis. We assume that integrated magnetic flux concentrators are layer-like (the planar dimensions of an MC are much larger than its thickness t). Moreover, since in practice we work only with very high-permeability materials, with $\mu_r > 10^5$, we assume $\mu_r \rightarrow \infty$.

3.1. Magnetic Gain

We define the magnetic gain of an MC as the ratio

$$G_{XY} = B_{HE} / B_0 \quad (1)$$

Here B_{HE} is the (perpendicular) component of the magnetic induction “seen” by the planar Hall element (HE) at a position (X,Y) (see Figure 1b)) and B_0 is the magnetic induction component parallel with the axis of the MC faraway from the MC.

Let us put the magnetic scalar potential difference (i.e. the equivalent excitation current I_{ex}) acting between the two adjacent MCs in the form

$$I_{ex} = KH_0(2L + g) \quad (2)$$

Here H_0 is the magnitude of the magnetic field vector H before introducing the MC, $H_0 = B_0 / \mu_0$. K is a numerical factor defined by $K = \int H_g dl / H_0 (2L + g)$, where H_g is the magnetic field in the gap and the integration is done over the gap. K tells us which part of the theoretically available equivalent excitation current along the whole length of the MC we can really use around the air gap. From physical arguments we estimate the limits for K in the two-dimensional case, with $L \gg t$, as follows: when $g/t \rightarrow 0$, then $K \approx g/t \rightarrow 0$; when $L \gg g \gg t$, then $K \approx 1/2$. The values of K deduced from numerical simulations, Figure 3, support these estimations.

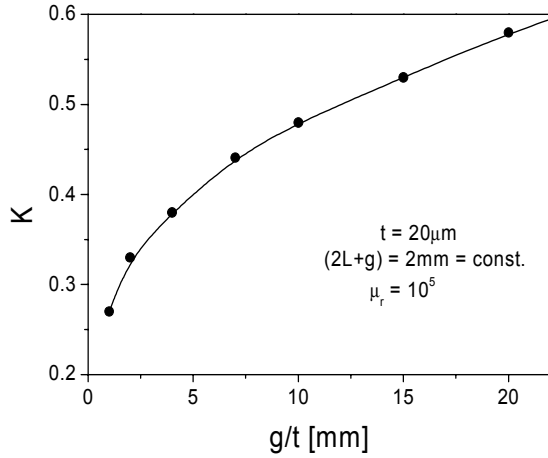


Figure 3 The values of the factor K deduced from two-dimensional simulation of twin planar MCs [8].

By inspecting Figure 2 we see that the magnetic field lines below the MC and close to the gap have approximately a circular form. This is a consequence of the boundary conditions. Using this fact we find now the magnetic gain of a twin MC for a HE placed at (X, Y) :

$$G_{XY} = \frac{K(2L+g)X}{\pi(X^2 + Y^2)} \quad (3)$$

for $X > g/2$, $g \approx t$ and $\mu_r \gg 1$

With an optimal layout of MC, for given t , L and g , one can increase K and so the magnetic gain G_{XY} up to a factor of 2 [13]. The realistic values of G_{XY} for an integrated sensor are between 5 and 10. But adding external MCs, this can be easily increased to about 100 [11].

3.2. Saturation Field

By inspecting Figure 2 we notice that the magnetic field lines have the highest density in the magnetic concentrators somewhere between the middle of each concentrator and the gap. We find the corresponding maximal magnetic flux density by calculating the total flux entering into an MC as follows:

$$B_{\max} \approx \mu_0 \frac{KH_0(2L+g)}{g} \left(1 + \frac{2}{\pi} \frac{g}{t} \ln(L/g)\right) \quad (4)$$

When this induction reaches the saturation induction B_{sat} of the MC material, our magnetic sensor shows a strong decrease in its magnetic sensitivity. The external magnetic field induction at the onset of the saturation is given by

$$B_{0sat} \approx B_{sat} g \left[K(2L+g) \left(1 + \frac{2}{\pi} \frac{g}{t} \ln(L/g)\right) \right]^{-1} \quad (5)$$

for $g \approx t$ and $\mu_r \gg 1$

For a sensor with the MCs of the total length $2L + g = 2$ mm, $t = g = 20$ μ m and $B_{sat} = 1$ T, we obtain $B_{0sat} \approx 10$ mT. By choosing an optimal form of the MC for given t , L and g , one can increase the saturation field up to a factor of 2 [12].

3.3. Device: a High-Sensitivity Single-Axis Integrated Hall Magnetic Sensor

By integrating twin magnetic concentrators with Hall elements, we obtain a magnetic sensor system with the following combination of features: existence of a magnetic gain, which brings a higher magnetic sensitivity, lower equivalent magnetic offset, and lower equivalent magnetic noise than those in conventional integrated Hall sensors; and sensitivity to a magnetic field parallel with the chip surface, much as in the case of magneto-resistance (MR) sensors. Figure 4 shows one example of such an integrated magnetic sensor.

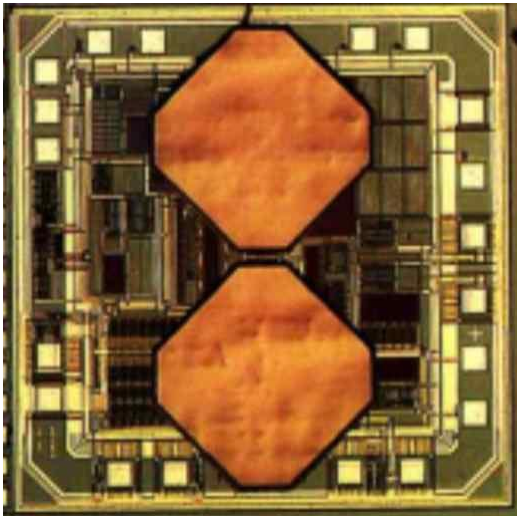


Figure 4 Photograph of an IMC Hall magnetic sensor chip (Sentron type 1SA-1M). The semiconductor part is a CMOS Hall ASIC. The twin magnetic concentrator has the form of the two octagons. The sensor responds to a magnetic field parallel with the in-plane symmetry axis through the two octagons. The magnetic sensitivity is programmable and can be as high as 300 V/T and the equivalent offset field is 0.03 mT. (Courtesy of SENTRON AG, Zug, Switzerland).

The electronic part of the magnetic sensor shown in figure 4 is realized in CMOS technology as a smart ASIC. The circuit includes biasing, amplification, cancelling offset, and temperature stabilization functions. The magnetic sensitivity, temperature coefficient of sensitivity, and residual offset of the sensor are programmable using the Zener-zapping technique.

3.4. Device: World Record Sensitivity

The sensitivity of a IMC Hall magnetic sensor can be further increased by attaching additional external flux concentrators to the integrated ones. In this way the sensitivity is increased by about one order of magnitude to 3000V/T and the field equivalent offset reduced to about 3 μ T (see Figure 5).

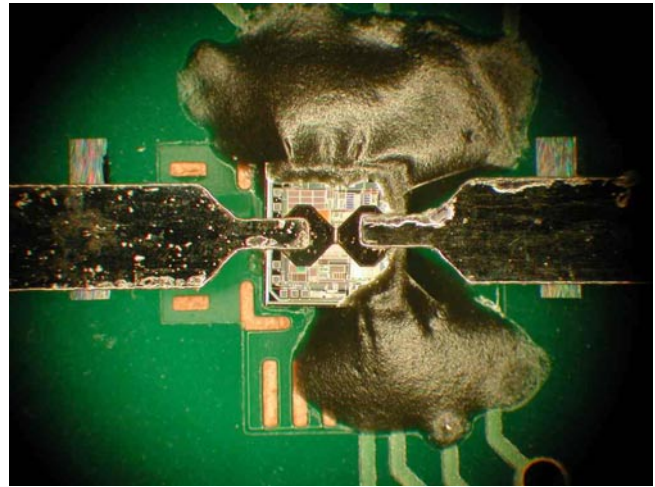


Figure 5 Photograph of an IMC Hall magnetic sensor chip (Sentron type 1SA-1M) with additional external flux concentrators. This device features world-record sensitivity of 3000V/T and a field equivalent offset of about 3 μ T.

The exact position of the external magnetic concentrators is not very critical, since the precise field shape around the Hall elements is given by the integrated ones. The only requirement is that the magnetic resistance between external and integrated flux concentrators is small compared to the magnetic resistance of the gap.

Such devices are used for magnetic tracking applications, where the position and orientation of a small-size permanent magnet is precisely determined within a certain volume by an array of these sensors [Ref Schlageter].

3.5. Performance Comparison

We shall now compare the characteristics of the first commercially available twin-IMC Hall ASIC (the Sentron type 1SA-1M [15]) with a few conventional single-axes magnetic field sensors.

Table 1 [9] shows the characteristics of three Hall ASICs (the Allegro BiCMOS type 3515, the Melexis CMOS type MLX90215, and the Sentron IMC/CMOS type 1SA-1M, described above). We notice that, thanks to the magnetic gain provided by the magnetic concentrator, the last (IMC) sensor features the highest magnetic sensitivity, the best resolution, and the largest bandwidth.

Table 1 Comparison of some Hall ASIC Single-Axis Magnetic Sensors

Technology →	BiCMOS	CMOS	IMC/CMOS	Unit
Sensor →	3515	MLX90215	1SA-1M	
Characteristics (*1) ↓				
a) Full Scale Field Range (FS)	+/- 40	+/- 14 (*2)	7 (*2)	mT
b) Sensitivity (typical)	50	140 (*2)	300 (*2)	mV/mT
c) Bandwidth (BW)	30	0.13	120	kHz
d) Linearity Error within FS	0.1	1	0.5	%FS
e) Hysteresis Error (+/-10 mT)	0	0	20	μT
f) Equivalent Offset at 300K	3	0.06 (*3)	0.45 (*3)	%FS
g) Offset TemCoef. Error	16	3	0.66 (*4)	μT/K
h) 1/f Noise Density at 1 Hz	0.3 (*5)	(*5), (*6)	0.3 (*5)	μT/√Hz
i) White Noise Density (*7)	0.2 (*5)	1.3 (*5)	0.03 (*5)	μT /√Hz
Resolution:				
j) For a quasi-DC field (*8)	167	67	31	μT
k) For low freq. fields (*9)	7	37	4.5	μT
l) For high freq. fields (*10)	0.2	1.3	0.03	μT

Notes (*):

- (1) At the supply voltage of 5V.
- (2) Programmable. The figure shows the optimal value for high resolution.
- (3) Quiescent output voltage is programmable. The figure shows the rest offset.
- (4) With the best programmed parameters.
- (5) Our own measurement.
- (6) Covered by the white noise.
- (7) Equivalent noise field at a sufficiently high frequency, beyond the 1/f region.
- (8) After zeroing the initial offset, within $\Delta T = 10K$: (j) = (e) + (g) ΔT + (k).
- (9) (k) = Peak to peak equivalent noise field: 7 x (rms noise field, $0.1 < f < 10Hz$).
- (10) For $BW \ll 1Hz$, we take (l) \approx (i) $\sqrt{1Hz}$. Otherwise, (l) is proportional to \sqrt{BW} .

Figure 6 shows the key performance data of the above Hall sensors and of two representative single-axis ferromagnetic thin-film magnetoresistance (MR) sensors [9].

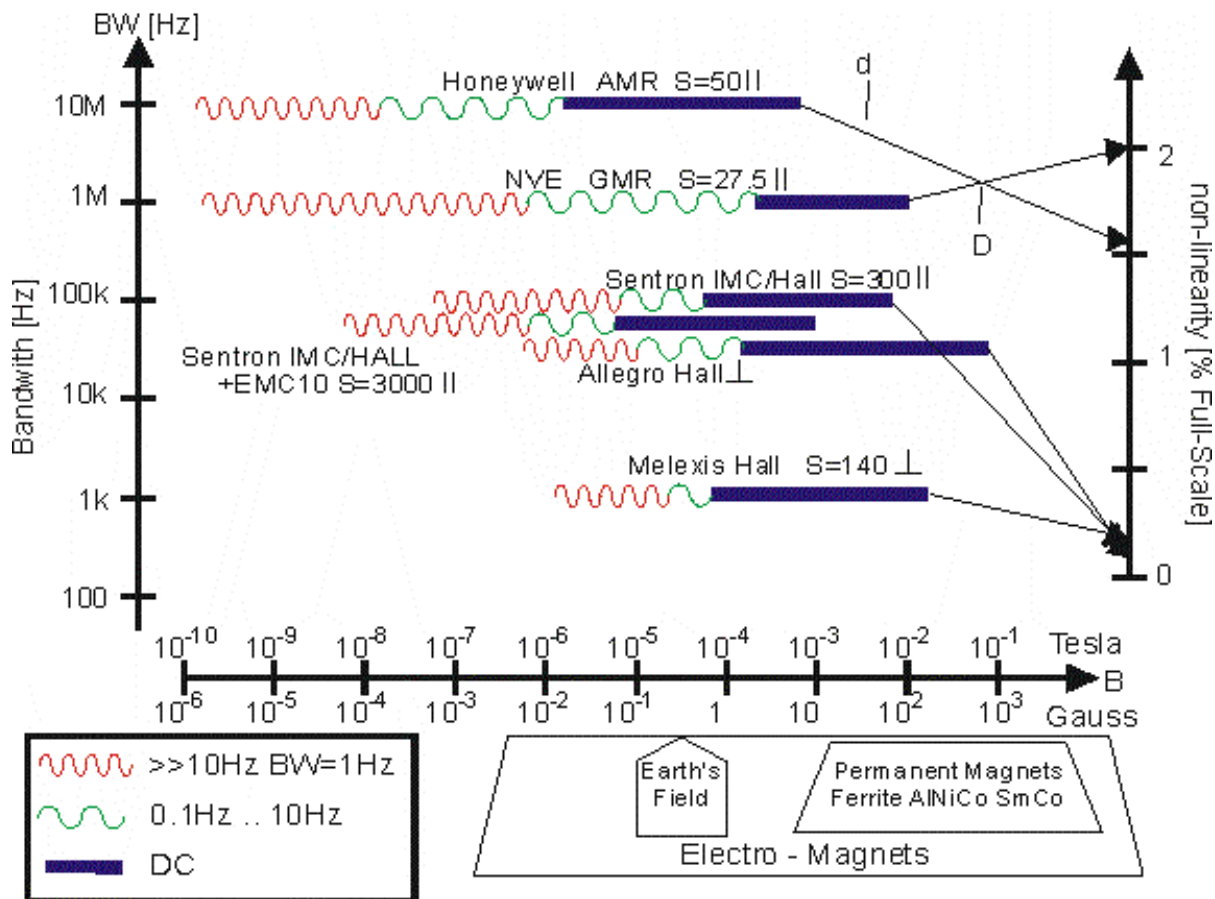


Figure 6 Key performance data of some AMR, GMR, and integrated Hall magnetic field sensors. MR performance are without Set/Reset offset reduction. Notation: The low-field limit of the lines denotes the detectivity limit (resolution) for DC field, low frequency field and high frequency field; The high field limit of the full lines denotes the full scale range; d: Disturbing field; D: Destroying field; S: Sensitivity at the supply voltage of 5V; ||: Sensitive to a field parallel with the chip surface; ⊥: Sensitive to a field perpendicular to the chip surface; +EMC10: with an additional, external, magnetic flux concentrator, providing a magnetic gain of 10 (see Figure 5).

By inspecting Figure 6, we conclude that the magnetoresistance sensors AMRs and GMRs are much better than modern Hall ASIC sensors only in the case of high-frequency AC magnetic measurements: then MRs are preferable for both higher resolution and larger bandwidth. But at low frequencies, the difference becomes smaller. For DC fields, an AMR or GMR are very good only if some kind of chopping (switching, set/reset) is applied (not shown in Figure 6); otherwise, the resolution of the IMC Hall ASIC is much better than that of GMR and approaches the resolution of a non-switched AMR.

concentrator converts locally a magnetic field parallel with the chip surface into a magnetic field perpendicular to the chip surface. The strongest perpendicular component of the magnetic field appears under the concentrator extremities. The Hall elements are placed under the concentrator extremities and “see” this perpendicular component of the magnetic field much as in the case of the twin magnetic concentrators.

4. SINGLE MAGNETIC FLUX CONCENTRATOR

A single integrated magnetic flux concentrator is shown in Figure 7 [16], [17]. Here again, the

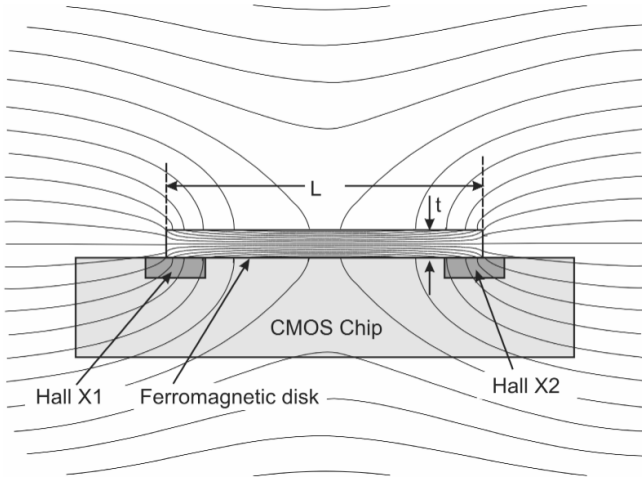


Figure 7 Cross-section of a Hall chip combined with a single magnetic flux concentrator. The magnetic concentrator usually has the form of a disc [17].

4.1. Magnetic Gain

We define the magnetic gain of a single magnetic flux concentrator in the same way as above, Eq. (1). In order to estimate the magnetic gain, we model a disk-like magnetic concentrator with an oblate ellipsoid. For a very flat oblate ellipsoid magnetized parallel to a long axis, the demagnetization factor [18] in our notation is

$$N \approx \frac{\pi}{4L} \left(1 - \frac{4t}{\pi L}\right) \quad \text{for } L/t \gg 1 \quad (6)$$

In a very high-permeability and not very elongated structure, the internal magnetic induction is

$$B_i \approx \frac{\mu_0}{N} H_0 \quad (7)$$

Assuming that the external magnetic induction “seen” by the Hall elements $B_{HE} \approx B_i$, we obtain for the magnetic gain

$$G_E \propto \frac{1}{N} \approx \frac{4}{\pi \frac{t}{L} - 4 \frac{t^2}{L^2}} \quad \text{for } \mu_r \rightarrow \infty \quad (8)$$

For a disc with $L/t = 10$, we calculate $G_E \approx 14.5$. Numerical simulations gave [17] a similar value for the total magnetic gain, but only about 7 for the perpendicular field component.

4.2. Saturation Field

From Eqs. (7) and (8) we readily obtain

$$B_{0sat} \approx B_{sat} / G_E \quad \text{for } \mu_r \rightarrow \infty \quad (9)$$

where B_{sat} is the saturation induction of the MC material. For a disk-like MC with $L/t = 10$ and $B_{sat} = 1$ T, this gives $B_{0sat} \approx 69$ mT.

4.3. Device: A Two-Axis Integrated Hall Magnetic Sensor

Figure 8 shows the structure of an integrated two-axes Hall magnetic sensor that uses the single magnetic flux concentrator described above [16]. The concentrator has the form of a thin disk. The Hall elements are positioned under the periphery of the disk. At least one Hall element per sensitive axis is needed; but preferably, for each sensitive axis we use two Hall elements placed at the two opposite ends of the disk diameter parallel with the corresponding axis. For example, for the component of a magnetic field collinear with the axis x in Fig. 2, we use the Hall elements Hall X1 and Hall X2.

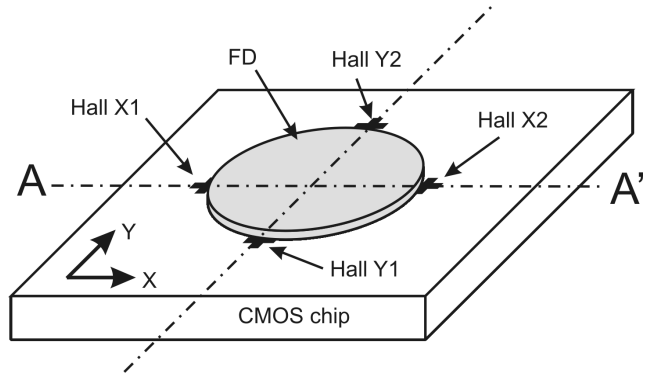


Figure 8 A schematic view of a two-axes Hall magnetic sensor. It consists of an integrated combination of a soft ferromagnetic disk (FD) and a few conventional Hall elements (Hall X1, X2, Y1, Y2) placed under the periphery of the disk. The role of the ferromagnetic disk is to convert an in-plane magnetic field into a perpendicular magnetic field, as illustrated in Figure 7.

With reference to Figure 7, the Hall element X1 “sees” a positive Z magnetic field component, whereas the Hall element X2 “sees” a negative Z magnetic field component. If we subtract the output voltages of the two Hall elements, we shall obtain a signal proportional to the mean value of the perpendicular components of the magnetic field at the two extremities of the ferromagnetic disk. Assuming a constant permeability of the disk and no saturation, the sensor output signal is proportional to the input (parallel) magnetic field.

According to (8), if the thickness t of a magnetic flux concentrator disk is much smaller than its diameter, then the magnetic field “seen” by the Hall elements is given by

$$B_H = C B_X L \quad (10)$$

Here C denotes a numerical coefficient; B_X is the input magnetic field induction, parallel with the chip plane; and L is the length of the magnetic flux concentrator collinear with the vector B_X . In other words, for a given external planar magnetic field B_X , the Hall voltage is proportional to the length of the magnetic flux concentrator.

Consider now what happens if the magnetic field acting on the sensor shown in Figure 8 rotates in the chip plane. Note first that, due to the rotational symmetry of the device, the form of the device “seen” by the magnetic field does not change with the rotation. Therefore, if the disk is made of a very “soft” ferromagnetic material, then the whole distribution of the magnetic field within and around the disk shall stay fixed and shall simply rotate synchronously with the rotation of the input magnetic field.

For simplicity, let us assume now that the Hall elements are positioned right at the peripheries of a disk, at the points A and B , Figure 9. If the input magnetic field vector B is collinear with the x -axis, the length of the magnetic flux concentrator associated with the Hall sensors at A and B is $AB = D$, where D denotes the diameter of the disk.

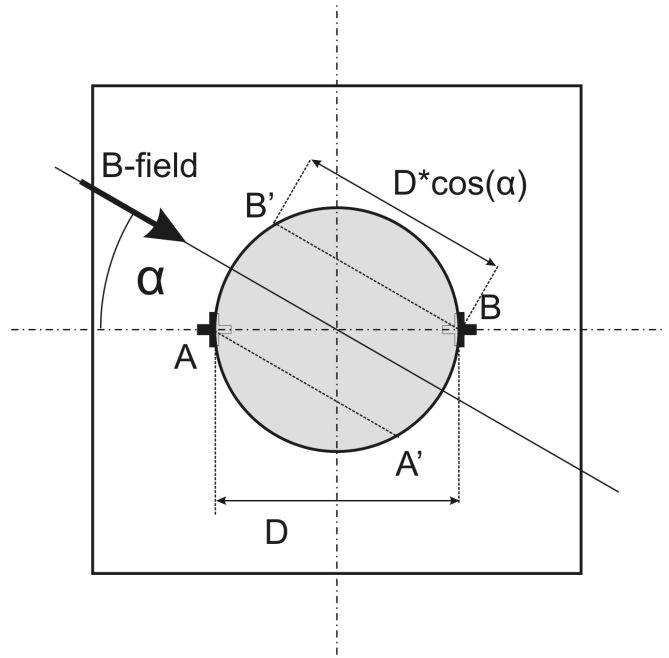


Figure 9 For a magnetic field vector rotated in the plane by an angle α with respect to the axis of the two Hall elements A and B , the original length of the concentrator ($A-B = D$) is reduced to ($A-A' = B-B'$). The effective length of the “new” concentrators is $D^* \cos(\alpha)$. Consequently the Hall voltages are also proportional with $\cos(\alpha)$.

But when the magnetic field rotates, the local lengths of the effective magnetic concentrators are given by the length of the sectors $A-A'$ and $B'-B$,

$$L = D \cos(\alpha) \quad (11)$$

By inserting this in (10), we obtain

$$B_H = C D B_X \cos(\alpha) \quad (12)$$

Then the difference of the Hall voltages of the two Hall elements Hall X1 and Hall X2 shall be given by

$$V_{HX} = 2 S C D B_X \cos(\alpha); \quad (13)$$

And the difference of the Hall voltages of the two Hall elements Hall Y1 and Hall Y2 shall be given by

$$V_{HY} = 2 S C D B_X \sin(\alpha) \quad (14)$$

Here S denotes the magnetic field sensitivity of the Hall elements.

From the two harmonic signals (13) and (14) phase-shifted by $\pi/2$, we can easily retrieve the information about the angular position of the magnetic field vector component parallel with the chip surface.

Figure 10 shows an integrated two-axis magnetic sensor based on this principle. The electronic part of the sensor is realized in CMOS technology as a smart ASIC. The circuit includes biasing, amplification, offset cancellation, and temperature stabilization functions. The residual offset of the sensor is programmable using the Zener-zapping technique. When used as a magnetic angular position sensor, this device provides, without any calibration, accuracy better than 0.5° over the measurement range of 360° .

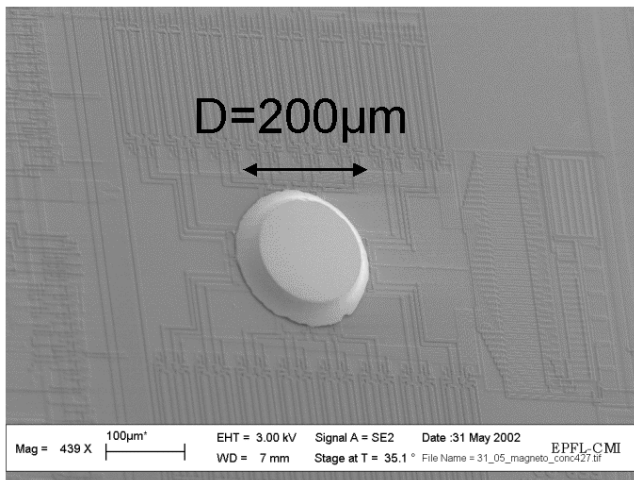


Figure 10 SEM photograph of an integrated IMC two-axis magnetic sensor (Sentron type 2SA-1). The semiconductor part is a CMOS Hall ASIC. The disk-like magnetic concentrator of $200\mu\text{m}$ diameter is deposited in a post-processing step. The sensor gives two components of an in-plane magnetic field and shall be used as an angular position sensor. (Courtesy of SENTRON AG, Zug, Switzerland).

5. APPLICATION EXAMPLES

5.1. Current Sensor

A single-axis Hall magnetic sensor ASIC with IMCs can be used in a very convenient way to measure the electrical current flowing through a conductor, without having to contact the conductor itself. The current through the conductor generates a magnetic field, which in turn is picked up by the flux concentrators of the sensor and, amplified, oriented toward the Hall elements. Two configurations of an IMC Hall Sensor and current conductor are of practical importance. For low current measurement ($<10\text{A}$), current conductor and Hall sensor are on the same printed circuit board (PCB) (Figure 11). For very low current, the conductor may even be realized

as several loops under the sensor to increase the generated magnetic field and with it the signal.

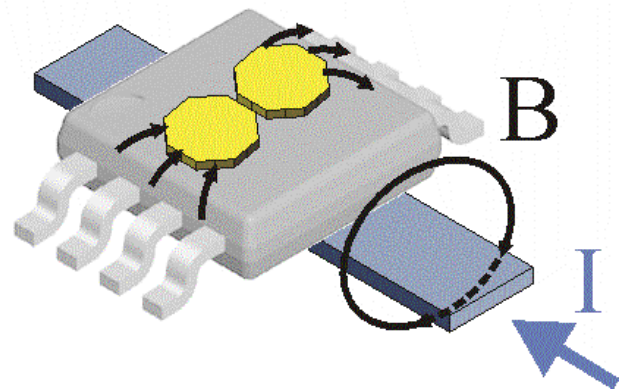


Figure 11 A flat stripe-like current conductor, e.g. a current track on the PCB underneath the chip, generates a magnetic field, which is collected by the magnetic flux concentrators. Such an implementation is particularly adapted for currents up to 10 Amperes.

Figure 12 shows how the signal amplitude is related to the current through the conductor with one, two, four and six loops of different conductor width under the chip.

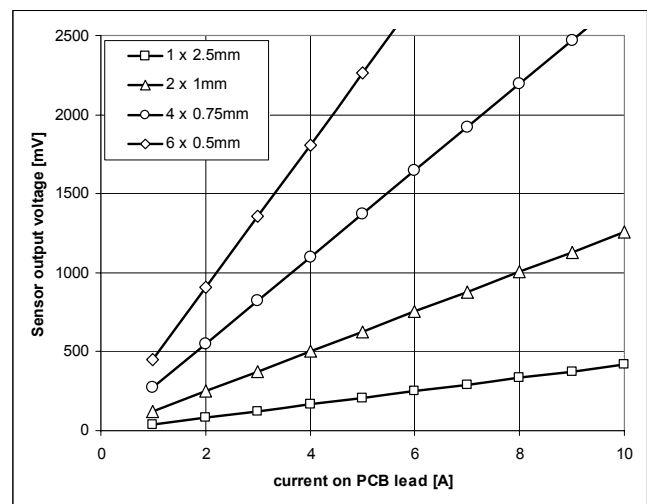


Figure 12 Sensor output as function of current on PCB conductor and number of current windings under the chip.

The second configuration for current measurement consists in mounting a conductor bar at a given distance from the current sensor (Figure 13). In such a way the conductor can be a solid copper lead supporting currents of 100 Amps or more (Figure 14).

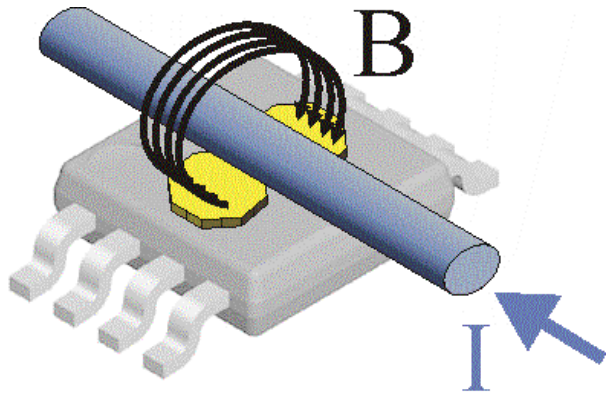


Figure 13 A current through a straight cylindrical conductor generates a cylindrical field. This field is collected by the magnetic flux concentrators, which amplify it on the Hall elements in the chip. This implementation is adapted for high current measurement, where the current conductor can be made of a solid copper bar.

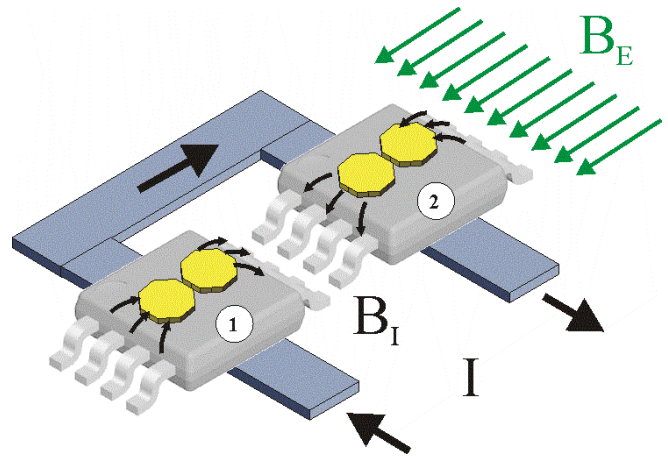


Figure 15 Two current sensors above a U-shape PCB current conductor see the magnetic field generated by the current B_I with opposite signs and an external parasitic field B_E with the same sign. By subtracting the output voltages (differential measurement) the influence of the external field is suppressed.

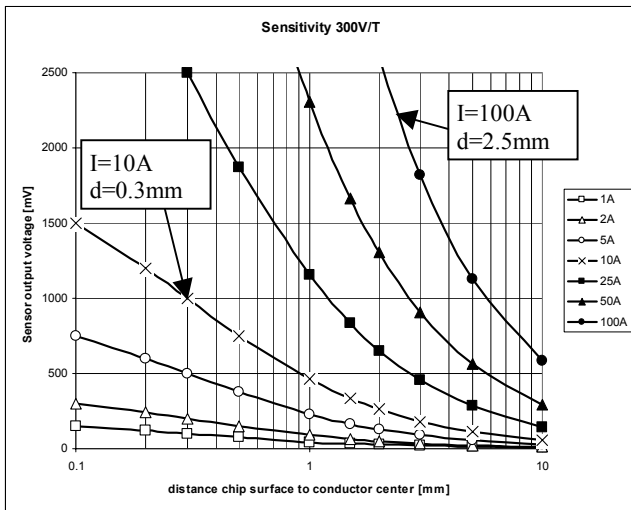


Figure 14 Sensor output voltage depending on current and distance between current lead and sensor surface.

Any deterioration of a precise current measurement by external magnetic fields (e.g. motor stray fields), can be efficiently reduced by differential current measurement. A practical solution is shown in Figure 15, where two current sensors are mounted over a U-shape PCB conductor. Both sensors “see” the current magnetic field B_I with opposite signs and an external magnetic field B_E with the same sign. Connecting the both sensor output pins as differential wires to a voltmeter increases the output signal and virtually suppresses the perturbation field.

5.2. Angular Position Sensor

A typical application for two-axis integrated Hall magnetic sensors is the contactless sensing of the angular position of a rotating shaft. For this application, as shown in Figure 16, a small magnet is mounted at the end of a rotating shaft above the sensor. Practical values are magnet diameters of a few millimeters and distances of some tenths of a millimeter to a few millimeters. The magnet generates a field that is rotating in the sensor plane with the shaft. Contrary to common Hall sensors this principle allows for very crude mounting tolerances without deteriorating the measurement accuracy, since the magnetic field is very homogenous in the area where the sensor is placed.

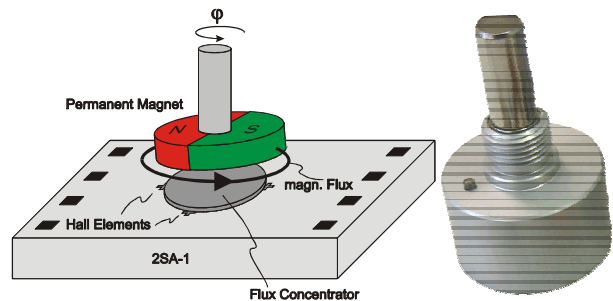


Figure 16 A two-axis integrated Hall magnetic sensor and a small magnet with magnetization parallel with the chip surface, mounted on a rotating shaft, combine to an angular position sensor (left). This principle is for example used in contactless potentiometers (right).

An example for this application is shown on the right: A contactless, wear-free full 360° potentiometer. A measurement showing accuracy and resolution of such a system is given in Figure 17. Since the angular information depends only upon the ratio of the two output signals X and Y , the system is virtually immune to any variation of the magnetic field strength (magnet ageing) or to any drift of the sensitivity (temperature effects), thus making it very robust.

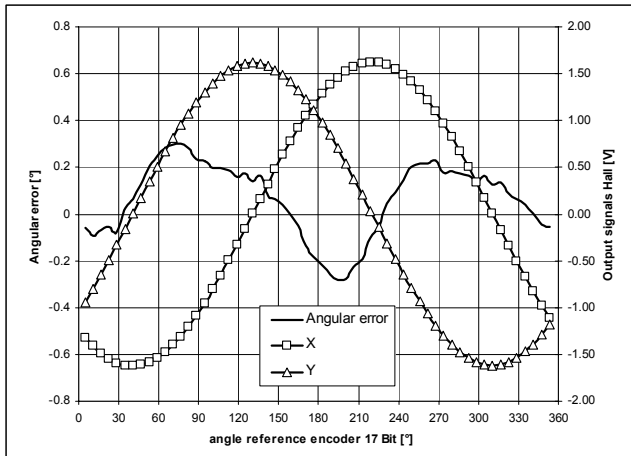


Figure 17 X and Y sensor output voltages and angular error of a magnetic angular position sensor realized with the chip shown in Figure 10. Over the full 360° rotation the accuracy is about 0.3° and the resolution better than 0.05°. The remaining error arises mostly from sensitivity mismatch between the two measurement axes, which is about 0.5%. A magnet with a diameter of 6mm at a distance of 4mm was used. It generates a field component parallel with the chip surface of about 16mT.

The two-axis integrated Hall device can also be used as a low-cost and reliable sensor in detecting the two-axis inclination of a manual control device (joystick) (Figure 18).

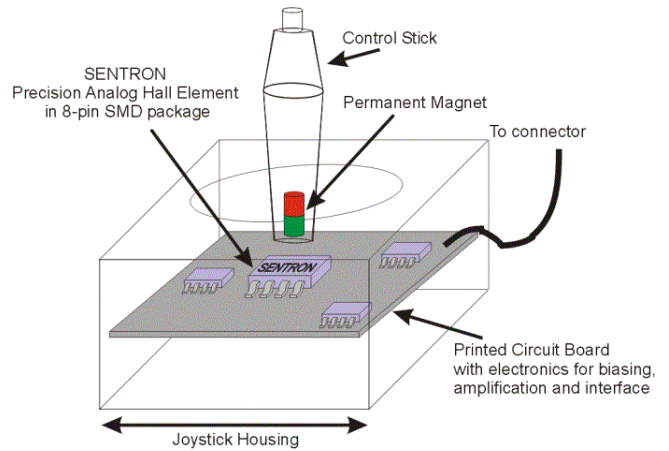


Figure 18 A two-axis Hall magnetic sensor and a small magnet with magnetization perpendicular to the chip surface combine to a two-axis inclination sensor that can, for example, be used in a contactless joystick.

This application takes particular advantage from the fact that the field component perpendicular to the chip surface adds to zero for each pair of Hall elements placed on opposite position under the edge of the ferromagnetic disk. The sensor output voltages are directly proportional to the inclination angles.

Another important application of angular position sensors is the signal generation for coil current commutation inside of small brushless DC motors. This allows to optimize motor efficiency and torque for large ranges of rotation speed and load. Contrary to the conventional solution, which require a separate Hall plate for each motor phase, an integrated Hall Sensor with IMC can provide all necessary signals from one chip.

6. CONCLUSIONS

We described in this paper a new family of integrated Hall magnetic sensors based on the technology of Integrated Magnetic Concentrators (IMC). The IMC Hall sensors respond to a magnetic field parallel to the chip surface and not, as conventional Hall magnetic sensors, to a field perpendicular to the chip surface.

The presence of IMC not only changes the geometry of the sensor positioning, but it also boosts the sensor performance and opens up the way to integrating additional functionality.

Thanks to the flux concentration effect, IMC Hall sensors have higher magnetic sensitivity, lower equivalent magnetic offset, and lower equivalent

magnetic noise than conventional Hall devices. Therefore, from the application point of view, these new integrated Hall sensors are similar to hypothetical low-offset and very linear magnetoresistive (MR) sensors. The key performance of the IMC Hall sensors are positioned somewhere between those of MRs and traditional Hall ASICs. Therefore, the IMC technology bridges the gap between AMRs, GMRs, and the conventional Hall ASIC magnetic field sensors.

Moreover, the structure of the IMC Hall sensors is fully compatible with conventional CMOS technology. This allows full system integration on a chip.

Typical applications of these new sensors include sensitive position sensing, current sensing, and contactless angle measurement.

7. REFERENCES

- [1] L. M. Ross et al., "Applications of InSb", *J. Electronics*, Vol. 2, 1955, pp. 223
- [2] H. Hieronymus et al., "Über die Messung kleinster magnetischer felder mit Hallgeneratoren", *Siemens – Z.*, 31, 1957, pp. 404-409.
- [3] M. Epstein et al., "Magnetic field pickup for low-frequency radio-interference measuring sets", *IRE Transactions on electron devices*, January 1961, pp. 70-77
- [4] P. A. Nazarov et al., "On selection of magnetic circuit for Hall effect devices", *Electric Technology USSR*, No. 1 (1981) 69-77.
- [5] See Fig. 6 in: R. S. Popovic, "Hall-effect devices" *Sensors and Actuators*, 17, 1989, pp. 39-53
- [6] A H Marchant, "Hall-effect devices for relay and other applications" *Electrotechnology*, July 1984, pp. 122-125.
- [7] R. S. Popovic et al., "Magnetfeldsensor", Swiss patent CH 659 896 A5, application date: 22.11.1982.
- [8] R.S. Popovic, P.M. Drljaca, C. Schott, R. Racz, "Integrated Hall Sensor / Flux Concentrator Microsystems", Invited Lecture, *37th International Conference On Microelectronics, Devices And Materials, MIDEM 01*, Bohinj, Slovenia, October 2001
- [9] R.S. Popovic, P.M. Drljaca, C. Schott, "Bridging The Gap Between AMR, GMR, And Hall Magnetic Sensors", Invited Lecture, *Proc. 23rd Int. Conference On Microelectronics (MIEL 2002)*, Vol. 1, Nis, Yugoslavia, 12-15 MAY, 2002, pp. 55-58
- [10] R. S. Popovic et al., US patents 5,942,895 and 6,184,679
- [11] P. M. Drljaca et al., "High Sensitivity Hall Magnetic Sensors Using Planar Micro and Macro Flux Concentrators", *Proc. of TRANSDUCERS '01*, Munich, Germany, June 2001
- [12] R. S. Popovic et al., "Integrated Hall-effect magnetic sensors", *Sensors and Actuators A*, Vol. 91, 2001, pp. 46-50.
- [13] P. M. Drljaca et al., "Design of Planar Magnetic Concentrators For High Sensitivity Hall Devices", *Sensors and Actuators A*, Physical, Vol. 97, pp. 10-14, April 2002
- [14] V. Schlageter, P. Drljaca, R. S. Popovic, P. Kucera, "A Magnetic Tracking System based on Highly Sensitive Integrated Hall Sensors", *Proc. MIPRO Conference*, Opatija, Croatia, 20-24 May, 2002
- [15] For details on commercially available IMC Hall magnetic sensors, see: www.sentron.ch.
- [16] Swiss Patent Application 2000 1645/00.
- [17] R. S. Popovic et al., "A new CMOS Hall angular Position sensor", *tm – Technisches Messen*, 68, June 2001, pp. 286-291.
- [18] R. C. O'Handley, *Modern magnetic materials*, John Wiley & Sons, Inc. 2000, Section 2.3.